Opt Quant Electron (2009) 41:771–777
DOI 10.1007/s11082-010-9390-2

# Investigation of geometrical effects of antireflective subwavelength grating structures for optical device applications

**Young Min Song · Yong Tak Lee**

Received: 5 October 2009 / Accepted: 5 May 2010 / Published online: 19 June 2010


**Abstract** We calculated diffraction efficiencies of subwavelength grating (SWG) structures for various optical device applications by using a rigorous coupled-wave analysis method. The geometrical effects, such as grating shape, height, and period, were investigated in order to obtain better antireflection performance. Cone shaped SWG structures with a taller height provide lower reflectance over a broadband wavelength range compared to that of flat surface and nanorod. It was found that the low reflection regions are quite related with the grating period and the refractive index of substrate materials. From the comparison between external and internal reflection of SWG structures, we also showed that the internal reflection requires shorter grating period than the case of external reflection to acquire broadband antireflection properties.

**Keywords** Subwavelength grating · Antireflection · Optical device · Effective medium theory · Nanostructure

## 1 Introduction

The phenomenon of antireflection is widely used to reduce optical losses at the interface between different optical media. Single or multi layer coatings are commonly used on various optical devices, such as solar cells, photodetectors, displays and viewing glasses, to suppress undesired reflections. However, thin film technology has inherent problems such as adhesion, thermal mismatch, and the stability of the thin film stack (Lalanne and Morris 1996; Walheim et al. 1999). Recently, subwavelength grating (SWG) structures,

Y. M. Song · Y. T. Lee
Department of Information and Communications, Gwangju Institute of Science and Technology, 1 Oryong-dong, Buk-gu, Gwangju, 500-712 Korea

Y. T. Lee (✉)
Department of Nanobio Materials and Electronics, Graduate Program of Photonics and Applied Physics, Gwangju Institute of Science and Technology, 1 Oryong-dong, Buk-gu, Gwangju, 500-712 Korea
e-mail: ytlee@gist.ac.kr

which are originated from the corneal of the night active insects, have been considered as a promising candidate for high-efficiency optical devices due to their broadband and omnidirectional antireflection properties (Kanamori et al. 1999; Yu et al. 2003; Striemer and Fauchet 2002; Huang et al. 2007; Song et al. 2009). The operation of SWG structures is understood easily in terms of a surface layer in which their refractive index varies gradually from 1.0 (air) to that of the bulk material. Therefore, Fresnel reflection can be reduced significantly by SWG structures with tapered features.

In order to obtain broadband antireflection property, the SWG patterns should have tapered profile, such as pyramidal and conical shape, with taller height. Many different methods, including e-beam or holographic lithography followed by dry etching (Kanamori et al. 1999; Song et al. 2009; Kintaka et al. 2001), colloidal formation (Sun et al. 2007, 2008), dynamic etching (Striemer and Fauchet 2002), and self-mask formation (Hsu et al. 2004; Huang et al. 2007), are used for the fabrication of SWG structures. However, it is clear that perfect cone or pyramid with very tall features would be costly in most of optical device applications. The shorter period also causes the process difficulty. Hence, it is mandatory to optimize the SWG structures geometrically for specific applications. In this study, we have calculated the reflection efficiency of the three kinds of SWG structures, i.e., nanorod, truncated cone, and perfect cone. Optimum structures are discussed in terms of reflectance and grating structures, such as the grating period and height. Moreover, the reflectance of the SWG structures is shown in case of the internal and the external reflection, together with the discussion for device applications.

## 2 Simulation results and discussion

Figure 1 show schematic illustrations of SWG structures for the reflectance calculation in shape of (a) nanorod, (b) truncated cone and (c) perfect cone. The theoretical calculations of the reflectance were done by using a rigorous coupled-wave analysis (RCWA) method proposed by Moharam (Moharam and Gaylord 1981, 1983). RCWA represents the electromagnetic fields as a sum over coupled waves. A periodic permittivity function is represented using Fourier harmonics. Each coupled wave is related to a Fourier harmonic, allowing

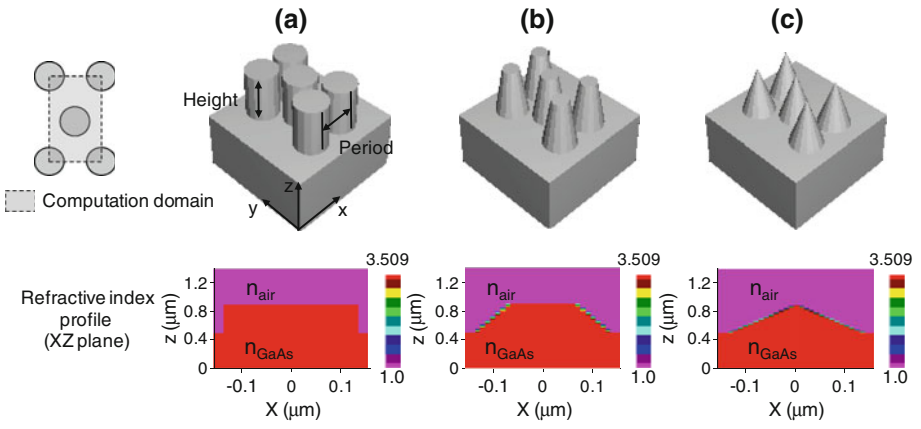


**Fig. 1** Schematic illustrations of SWG structures on GaAs in shape of (**a**) nanorod, (**b**) truncated cone and (**c**) perfect cone used in reflectance calculation

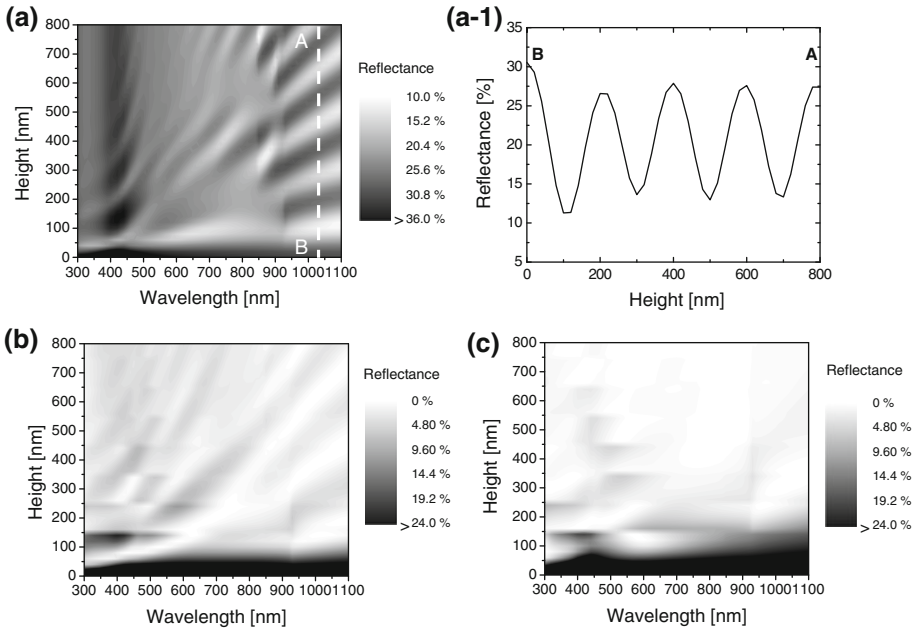


**Fig. 2** Contour plot of the variation of reflectance of SWG structures in shape of (**a**) nanorod, (**b**) truncated cone and (**c**) perfect cone as a function of height and wavelength for a 300 nm period. (a-1) Reflectance variations along *dashed line* AB of (**a**)

the full vectorial Maxwell's equations to be solved in the Fourier domain. The diffraction efficiencies are then calculated at the end of simulation in order to obtain the total reflectance. In this calculation, the period was fixed at 300 nm and the height was varied from 0 to 800 nm. To enlarge the packing density, 6-fold hexagonal symmetry was used, and the gap between each pillars were fixed to 10% of the period. The apex diameter was set to 50% of the base diameter in the truncated cone. The GaAs was used as a substrate material, which is widely used in highly efficient concentrator solar cells and other optoelectronic devices. The dispersion and absorption of GaAs was considered to calculate the exact reflectance at each wavelength (Palik 1991). All calculations were conducted at normal incidence angle.

Figure 2 shows the contour plot of the variation of reflectance of SWG structures in shape of (a) nanorod, (b) truncated cone and (c) perfect cone as a function of height and wavelength for a 300 nm period. In case of nanorod structure, because the nanorod acts as an effective medium that approximates a single layer thin film, the reflectance is not much smaller than that of flat surface. The optical properties of the nanorod with subwavelength period are quite similar with that of single layer antireflection coating. As shown in Fig. (a-1), the ripple pattern occurs due to the interference of light reflected at the top and bottom of the layer. The distance from peak to peak depends on the effective refractive index of nanorod. Since the nanorod with subwavelength period shows low reflectance only specific wavelength ranges, this design is not adequate for broadband applications.

As shown in Fig. 2b and c, the conical shape has lower reflectance than that of flat surface or nanorod. As the height is increased, the reflectance tends to decrease, because the effective index is more slowly changed. For example, the perfect cone provides very low reflectance (below 1%) over a wide spectral range at cone heights above 600 nm. Even though the

truncated cone has a tapered profile, the reflectance is higher than that of the perfect cone due to the index discontinuity between the air and the apex of the cone. However, the truncated cone with a short height (below 250 nm) has lower reflectance than that of the perfect cone at specific region. This means that, for a specific application there are no need the perfect cone, which cause complex process steps. The cone height and shape can be chosen according to this plot.

In conventional grating structure, the grating period is crucial to determine the diffraction angle and angular dispersion (Hecht 2002). On the other hand, in the SWG structures, it is difficult to predict the effect of the grating period, because these structures act as an effective medium. Therefore, it is worthwhile to find out some tendency between the grating period and the reflectance using the theoretical calculation. Figure 3 shows the influence of the period on the reflectance as a function of the wavelength for the SWG structures with the refractive index of (a) 3.5, (b) 2.5, (c) 1.5, (d) Silicon, (e) GaAs and (f) GaN. First, to clarify the effect of the period, the refractive index was fixed to constant value at whole wavelength ranges. As shown in Fig. 3(a), the low reflectance band broadens and shifts towards a higher wavelength region as the grating period increase. Figure 3b and c show also similar tendency, but their gradient and position is different each other.

For the qualitative analysis, we assumed that these low reflectance band has a linear relationship, which is defined by;

$$P_{opt} = A \cdot \lambda + B \tag{1}$$

where $P_{opt}$ is the optimum period for reflection minima, $\lambda$ is wavelength, $A$ is the gradient and $B$ is the $y$-intercept, respectively. We chose two points as an initial and final position to deduce the gradient and the $y$-intercept of each low reflectance band. As shown in Table 1, the gradient of the linear function with higher refractive index has higher values than that of low refractive index, which implies that the optimum period is rapidly increased as the wavelength increase. By applying the refractive index of semiconductor materials (silicon, GaAs, GaN) considering with the dispersion, similar contour plots were obtained. Contour plots for the case of silicon and GaAs are close to Fig. 3a, but higher reflection region is little bit different due to different refractive index spectra. The contour plot of GaN is similar with Fig. 3b. In Fig. 3e, for periods above 300 nm, the band splits into two bands with reflectance of <0.5%, including a band which is independent of the period of 200–450 nm at wavelength around 610 nm. This indicates that low reflectance in a specific wavelength range can be obtained by adjusting the cone height without changing its period.

Some optical devices such as light-emitting diodes and display panels emit light from inside to outside. In that case, the internal reflection, which means the refractive index of the incident medium is higher than that of transmitting medium, should be considered. When the light is incident on SWG structures with period $\Lambda$, the angles of the transmitted diffraction waves $\theta_{t,m}$ in the $m$-th diffraction order are given by the grating equation (Hecht 2002),

$$\sin\theta_{t,m} = \frac{m\lambda}{\Lambda n_2} + \frac{n_1}{n_2}\sin\theta_i \tag{2}$$

where $n_1$ and $n_2$ are the refractive indices of the incident and the transmitting medium, respectively, $\theta_i$ is the incidence angle, and $\lambda$ is the incident wavelength. In external reflection, if the period of the diffraction grating becomes much smaller than the optical wavelength, only zeroth order is allowed to propagate. Unlike the external reflection, it is difficult to satisfy the zeroth order condition in the internal reflection due to higher refractive index of incident medium.

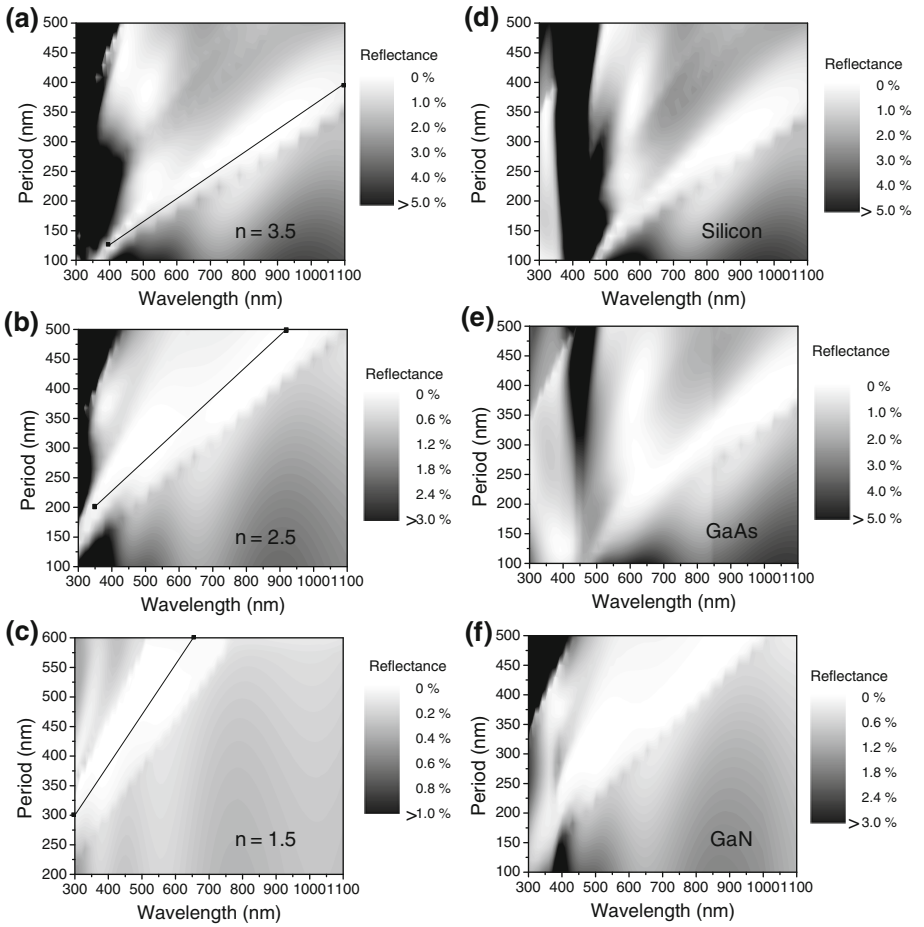


**Fig. 3** Contour plot of the influence of the period on the reflectance as a function of the wavelength for the SWG structures with the refractive index of (**a**) 3.5, (**b**) 2.5, (**c**) 1.5, (**d**) Silicon, (**e**) GaAs and (**f**) GaN

**Table 1** Gradient and *y*-intercept of the optimum period for SWG structures with different refractive index

| Refractive index | Initial position | Final position | A | B |
|---|---|---|---|---|
| $n = 3.5$ | (400, 125) | (1100, 400) | 0.392 | −31.8 |
| $n = 2.5$ | (350, 200) | (925, 500) | 0.522 | 17.3 |
| $n = 1.5$ | (300, 300) | (650, 600) | 0.857 | 192.9 |

Figure 4 shows the reflectance of GaN SWG structures in case of external and internal reflection as a function of wavelength for the period of 200, 300, and 400 nm. As shown in Fig. 4, antireflection properties of <1% were obtained at wavelength above ~820 nm for the period of 400 nm. Higher order diffractions, however, occur at wavelength below ~820 nm in case of the internal reflection, which significantly increase the total reflectance. This is attributed to the higher refractive index of GaN (~2.5) compared to that of air (1.0), as expected in Eq. (2). Because the zeroth order condition is quite related with the grating period as well as the refractive index, the low reflectance regions extend as the period decreases. As shown in

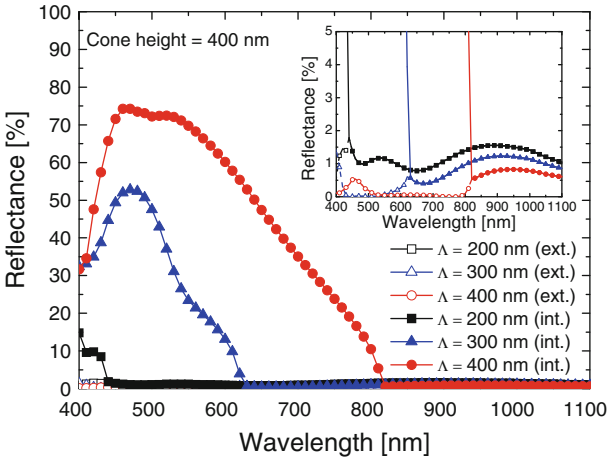


**Fig. 4** Reflectance of GaN SWG structures in case of external (*dash line*) and internal reflection (*solid line*) versus wavelength for the period of 200, 300, and 400 nm. Inset shows the magnified plots at 0–5% reflectance range

inset of Fig. 4, the reflection curve split at about 820, 630, and 440 nm for the period of 400, 300, and 200 nm, respectively. According to Eq. (2), longer periods with higher refractive index of incident medium generate higher order diffraction, which disturbs efficient anti-reflection in grating structures. In order to obtain low reflectance in light emitting devices, hence, the period of the diffraction grating should be much shorter than the case of external reflection.

## 3 Conclusion

Three kinds of SWG structures were used to simulate the diffraction efficiency and the structural optimization was discussed for optical device applications. From the contour plots, the effects of the cone heights and periods on the reflectance were also analyzed. It was found that the grating period and the refractive index is closely related with the low reflection band. The comparison between internal and external reflection was conducted for applying the SWG structures to light emitting devices. We expect that these calculation results are very helpful to design the SWG structures for various optical device applications.

**Acknowledgment** This research was partly supported by the IT R&D program of MKE/IITA [2007-F-045-03], by the GIST Systems Biology Infrastructure Establishment Grant, by the World Class University (WCU) program at GIST through a grant provided by MEST of Korea (R31-20008-000-10026-0), and by the Core Technology Development Program for Next-generation Solar Cells of Research Institute for Solar and Sustainable Energies (RISE), GIST.

## References

Hecht, E.: Optic, 4th edn. Addison Wesley, San Francisco (2002)

Hsu, C.-H., Lo, H.-C., Chen, C.-F., Wu, C.T., Hwang, J.-S., Das, D., Tsai, J., Chen, L.-C., Chen, K.-H.: Generally applicable self-masked dry etching technique for nanotip array fabrication. Nano Lett. **4**, 471–475 (2004)

Huang, Y.-F., Chattopadhyay, S., Jen, Y.-J., Peng, C-Y., Liu, T.-A., Hsu, Y.-K., Pan, C.-L., Lo, H.-C., Shu, C.-H., Chang, Y.-H., Lee, C.-S., Chen, K.-H., Chen, L.-C.: Improved broadband and quasi-omnidirectional anti-reflection properties with biomimetic silicon nanostructures. Nature Nanotechnol. **2**, 770–774 (2007)

Kanamori, Y., Sasaki, M., Hane, K.: Broadband antireflection gratings fabricated upon silicon substrate. Opt. Lett. **24**, 1422–1424 (1999)

Kintaka, K., Nishii, J., Mizutani, A., Kikuta, H., Nakano, H.: Antireflection microstructures fabricated upon fluorine-doped $SiO_2$ films. Opt. Lett. **26**, 1642–1644 (2001)

Lalanne, P., Morris, G.M.: Design, fabrication and characterization of subwavelength periodic structures for semiconductor anti-reflection coating in the visible domain. Proc. SPIE **2776**, 300–309 (1996)

Moharam, M.G., Gaylord, T.K.: Rigorous coupled-wave analysis of planar-grating diffraction. J. Opt. Soc. Am. **71**, 811–818 (1981)

Moharam, M.G., Gaylord, T.K.: Three-dimensional vector coupled-wave analysis of planar-grating diffraction. J. Opt. Soc. Am. **73**, 1105–1112 (1983)

Palik, E.D.: Handbook of Optical Constants of Solids II. Academic, London (1991)

Song, Y.M., Bae, S.Y., Yu, J.S., Lee, Y.T.: Closely packed and aspect-ratio controlled antireflection subwavelength gratings on GaAs using a lens like shape transfer. Opt. Lett. **34**, 1702–1704 (2009)

Striemer, C.C., Fauchet, P.M.: Dynamic etching of silicon for broadband antireflection applications. Appl. Phys. Lett. **81**, 2980–2982 (2002)

Sun, C.-H., Min, W.-L., Linn, N.C., Jiang, P., Jiang, B.: Templated fabrication of large area subwavelength antireflection gratings on silicon. Appl. Phys. Lett. **91**, 231105 (2007)

Sun, C.-H., Ho, B.J., Jiang, P., Jiang, B.: Biomimetic subwavelength antireflective gratings on GaAs. Opt. Lett. **33**, 2224–2226 (2008)

Walheim, S., Schaffer, E., Mlynek, J., Steiner, U.: Nanophase-separated polymer films as high-performance antireflection coatings. Science **283**, 520–522 (1999)

Yu, Z., Gao, H., Wu, W., Ge, H., Chou, S.T.: Fabrication of large area subwavelength antireflection structures on Si using trilayer resist nanoimprint lithography and liftoff. J. Vac. Sci. Technol. B **21**, 2874–2877 (2003)